International Journal of Nanomedicine

Dovepress
open access to scientific and medical research

Open Access Full Text Article

ORIGINAL RESEARCH

Facilitated and Controlled Strontium Ranelate Delivery Using GCS-HA Nanocarriers Embedded into PEGDA Coupled with Decortication Driven Spinal Regeneration

Chih-Wei Chiang[1,2,*]
Chih-Hwa Chen[3–6,*]
Yankuba B Manga[4]
Shao-Chan Huang[4]
Kun-Mao Chao[1,7]
Pei-Ru Jheng[4]
Pei-Chun Wong[4]
Batzaya Nyambat[4]
Mantosh Kumar Satapathy[4]
Er-Yuan Chuang[4,8]

[1]Graduate Institute of Biomedical Electronics and Bioinformatics, National Taiwan University, Taipei, 10617, Taiwan; [2]Department of Orthopedics, Taipei Medical University Hospital, Taipei, 11031, Taiwan; [3]Department of Orthopedics, Taipei Medical University–Shuang Ho Hospital, New Taipei City, 23561, Taiwan; [4]Graduate Institute of Biomedical Materials and Tissue Engineering, International PhD Program in Biomedical Engineering, School of Biomedical Engineering, College of Biomedical Engineering, Taipei Medical University, Taipei, 11031, Taiwan; [5]School of Medicine, College of Medicine, Taipei Medical University, Taipei, 11031, Taiwan; [6]Research Center of Biomedical Device, Taipei Medical University, Taipei, 11031, Taiwan; [7]Department of Computer Science and Information Engineering, National Taiwan University, Taipei, 10617, Taiwan; [8]Cell Physiology and Molecular Image Research Center, Taipei Medical University–Wan Fang Hospital, Taipei, 116, Taiwan

*These authors contributed equally to this work

Correspondence: Er-Yuan Chuang
Email eychuang@tmu.edu.tw

Background and Purpose: Strontium ranelate (SrR) is an oral pharmaceutical agent for osteoporosis. In recent years, numerous unwanted side effects of oral SrR have been revealed. Therefore, its clinical administration and applications are limited. Hereby, this study aims to develop, formulate, and characterize an effective SrR carrier system for spinal bone regeneration.

Methods: Herein, glycol chitosan with hyaluronic acid (HA)-based nanoformulation was used to encapsulate SrR nanoparticles (SrRNPs) through electrostatic interaction. Afterward, the poly(ethylene glycol) diacrylate (PEGDA)-based hydrogels were used to encapsulate pre-synthesized SrRNPs (SrRNPs-H). The scanning electron microscope (SEM), TEM, rheometer, Fourier-transform infrared spectroscopy (FTIR), and dynamic light scattering (DLS) were used to characterize prepared formulations. The rabbit osteoblast and a rat spinal decortication models were used to evaluate and assess the developed formulation biocompatibility and therapeutic efficacy.

Results: In vitro and in vivo studies for cytotoxicity and bone regeneration were conducted. The cell viability test showed that SrRNPs exerted no cytotoxic effects in osteoblast in vitro. Furthermore, in vivo analysis for new bone regeneration mechanism was carried out on rat decortication models. Radiographical and histological analysis suggested a higher level of bone regeneration in the SrRNPs-H-implanted groups than in the other experimental groups.

Conclusion: Local administration of the newly developed formulated SrR could be a promising alternative therapy to enhance bone regeneration in bone-defect sites in future clinical applications.

Keywords: strontium ranelate, drug formulation, nanoparticles, hyaluronic acid, glycol chitosan

Introduction

Bone graft substitutes have been improved with advanced bone graft materials for significant bone regeneration in orthopedic applications. Conventional orthopedic surgical procedures such as spinal fusion, revised fracture, non-union, and bone tumor removal, require bone graft substitutes to improve the surgical outcome. More specifically, spinal fusion is an important surgical procedure[1] that helps reduce pain by restoring defective spine stability. Advanced spinal fusion techniques use suitable bioinspired bone graft materials to improve the fusion process,

Received: 4 August 2020
Accepted: 3 March 2021
Published: 22 June 2021

including allografts, autografts, and synthetic bone substitutes.[2] Autografts have emerged prominently in bone formation owing to their excellent osteoconductivity, osteoinductivity, and osteogenesis. However, autograft transplantation has clinical limitations, such as donor-site morbidity.[3] Furthermore, contamination, immune rejection, and infection are significant drawbacks of their transplantation.[3] Hence, the development of ideal biocompatible materials for bone tissue regeneration is essential in orthopedics tissue engineering.

In light of the above-mentioned issue, strontium ranelate (SrR) is an oral medication with distinctive dual pharmacological properties for suppressing bone resorption and enhancing bone formation.[4] Thus, it is also used to prevent bone loss, increase bone strength, and decrease fracture risks.[5] Furthermore, SrR can reduce the risk of vertebral and non-vertebral fractures in postmenopausal women.[5] SrR has long been prescribed as a potent oral medication in orthopedic clinics.[6] However, it shows low systemic bioavailability, which might result in poor efficacy and adverse side effects such as headaches, nausea, diarrhea, gastrointestinal discomfort, skin allergies such as eczema and dermatitis. Recently, the European medicine agency has issued a legal warning on the oral administration and clinical application of SrR, leading to additional monitoring for high-risk deep vein thrombosis, cardiac failure, and any potential unwanted adverse effects.[7,8] Moreover, an effective and safer drug delivery to avoid systemic side effects[6] is highly recommended. Site-specific local delivery would be a better choice for promoting bone regeneration[9,10] owing to its recent clinical advancement for osteoporosis and fracture treatment via slow-release,[6] which prevents severe cardiovascular risks and adverse effects.[11] In due course, this therapeutic approach may bypass intestinal and hepatic first-pass metabolism for oral administration, thereby enhancing drug efficacy.

According to a previously published article, SrR-loaded chitosan film promotes in vitro osteoblast proliferation and differentiation on the titanium surface.[9] Another research reported that the polycaprolactone-laponite scaffold developed for the encapsulation and controlled release of SrR could maintain in vitro cell viability and enhance ALP activity.[10] However, to the best of our knowledge, limited or rare research has been done on the developed multi-carriers for sustained release of encapsulated SrR on the preclinical safety, in vivo therapeutic efficacy for bone regeneration. Thereby, it is essential to clarify whether sustainably released SrR from drug carriers is biocompatible and therapeutically effective in vivo.

Cationic polysaccharide glycol chitosan (GCS) or chitosan[12] and its nanoformulations are excellent drug-carrier for delivery systems due to their suitable physicochemical features, biocompatibility, biodegradability, and mucoadhesiveness. Hydrophilic drugs, such as SrR, can also be efficiently nanoencapsulated with chitosan-based nanoparticles (NPs).[13] Furthermore, hyaluronic acid (HA)-based biomaterials[14] have been used extensively in receptor-mediated controlled-release and targeted drug delivery systems.[15,16] Recent studies have shown that osteocytes and osteoblasts express HA (and its receptor, such as CD44).[17] Hence, HA and GCS-based composite biomaterials could be used as a newly designed nanocarrier system for SrR encapsulation. Poly(ethylene glycol) diacrylate (PEGDA)[18] is classified by the US Food and Drug Administration as a safe polymeric material for clinical use. It can further be used as an efficient hydrogel scaffold system in tissue engineering.[19] Both natural and synthetic polymeric materials are generally used in drug delivery systems.[20] They can also be expected to provide adequate mechanical support for sustained drug release in maintaining a safe therapeutic concentration of active drug substance.

In this study, SrR was encapsulated in GCS/HA nanocarrier (SrRNPs). The developed SrRNPs were embedded into PEGDA-based hydrogels (SrRNPs-H) for site-specific local drug delivery to improve osteogenesis. Local administration of SrR should minimize the side effects.[21] The physicochemical characteristics of various test formulations and material–cell interactions were evaluated. The in vitro and in vivo bioavailability in inducing bone regeneration were analyzed.

Furthermore, we hypothesized that SrRNPs-H could enhance osteogenesis in a rat decortication model along with the site-specific slow release of SrR. The multiple carrier-delivery system was anticipated to be effective and safe for local administration, which will enable the enhancement of bone regeneration. Thus, these biocompatible polymeric nanocomposite hydrogels could stand out as an excellent and potential biomaterial for future orthopedic applications.

Experimental Section

Materials

Chemical-grade biomaterials HA (MW 41 kDa) and GCS were purchased from Long Chen Shing (Kaohsiung, Taiwan) and Sigma-Aldrich, respectively. Other reagents and chemicals used were of analytical grade and obtained

from Sigma-Aldrich, Uni-Onward Corp., Bioman Scientific Co. Ltd, ASIA Bioscience Co., Ltd, Thermo Fisher Scientific, and GeneDireX Inc., all from Taiwan.

Optimal Formulations and Characterization of SrRNPs

SrR, as an active drug, was loaded into GCS/HA NPs via a simple electrostatic interaction-mediated nanoformulation procedure. A similar finding was reported.[13] First, GCS in acetic acid and HA (deionized (DI) water) were subsequently and separately prepared. Further, the SrR powder was dispersed uniformly in the HA solution and then stirred at 600 rpm (room temperature) to acquire a solution of 0.1% (w/v) SrR in HA. Various concentrations of GCS solutions were added drop-by-drop to the above solution with continuous stirring until the mixture was cloudy, and the mixture was further stirred for 30 s. Various concentrations of GCS were obtained: very low (0.09 mg/mL), low (0.17 mg/mL), medium (0.32 mg/mL), high (0.44 mg/mL), and very high (0.55 mg/mL). Finally, the test concentrations of GCS were incorporated with SrR and HA solution mixture to develop the nanocomplex (SrRNPs).

In the stability test, SrRNPs were immersed into different pH phosphate-buffered saline (PBS). The pH and temperature of SrRNPs were evaluated by a pH meter (SUNTEX INSTRUMENTS, SP2300) and a thermocouple (LUTRON ELECTRONIC ENTERPRISE CO., LTD, TM-925). According to the published literature, storage temperature (4°C),[22] body temperature (37°C),[23] and biological environmental pH (6.0–7.4),[24] were usually designed for the carrier stability test. Thus, the stability test was performed in the given pHs and temperatures.

The dynamic light scattering and zeta potential data were measured using Malvern Zetasizer (Malvern Instruments, UK). The pH and temperature stability of SrRNPs were also evaluated. The micro-morphological characterization of the hydrogel scaffolds was examined by scanning electron microscopy (SEM) (SU3500; Hitachi, Tokyo, Japan) and transmission electron microscopy (TEM). SEM analysis was carried out at an attuned working distance and voltage of approximately 3 mm and 10 kV.

Fourier transform infrared spectroscopy (FTIR) (Nicolet iS50; Thermo Fisher Scientific) was used to characterize and observe the chemical properties and composition of the fabricated SrR-nanocomplex. The quantitative encapsulation efficiency of SrR was assessed using a microplate spectrophotometer, as per the previous article.[13] The amount of SrR in the NPs was determined by absorbance (320 nm). The supernatant was obtained from the process of SrRNPs centrifugation (10,000 rpm, 20 min) and analyzed by the absorbance approach developed and validated previously. The concentration of SrR in the supernatant was obtained by comparing the concentration to a created absorbance analytical curve. The amount of SrR embedded into the NPs was verified by subtracting the supernatant quantity from the total quantity utilized before centrifugation. The examination of encapsulation efficiency was conducted in triplicate.

Cellular Interactions

The osteoblasts were obtained from New Zealand (NZ) white rabbits (Wei-Hsin Co., Taiwan). The harvested osteoblasts were according to the previously published protocol. The NZ adult rabbits' bone was obtained after euthanasia, and tissues were minced into small parts and washed. Then, tissues were incubated in Dulbecco's Modified Eagle Medium (DMEM) and supplemented with 10% fetal bovine serum and 1% PSA at 37°C in a humidified incubator with 5% CO_2. Cells typically migrated from the tissues within 10–14 days and reached confluence at 3–4 weeks.[25]

Cellular interactions with the synthesized NPs were investigated by GCS labeling with Cy5-N-hydroxysuccinimide (NHS)-ester dye, as per a previous study.[26] The NHS ester on Cy5 could react with GCS in dimethyl sulfoxide in the absence of light. After the reaction was complete, the solution was dialyzed and purified fluorescent Cy5-NPs for further study. The NPs test samples intracellular uptake were examined, culturing the cells on coverslip of confocal dishes (1.0×10^4 cells/dish) and incubated till confluence. The dishes containing cells were then washed twice with fresh medium and treated with Cy5-NPs, or Cy5-NPs pretreated with HA (1 mg/mL, 1 h) as an HA receptor inhibitor medium, which was dispersed in the same medium. The cells were washed twice with PBS after an additional incubation for 120 min before microscopic analysis. Fluorescence microscopy was performed to visualize the morphology of cells counterstained with DAPI.

To examine intracellular alkaline metals' distribution after the internalization of metal particles (SrR), test samples (Control, SrR, NPs, and SrRNPs) were incubated with osteoblasts cells. Intracellular alkaline metals were qualitatively (microscopy) and quantitatively (absorbance spectroscopy) analyzed in cells stained with Alizarin red S (ARS). Stained samples were examined under an inverted phase-contrast

light microscope (Nikon Eclipse-Ti; Nikon Instruments, Melville, NY) and a microplate reader.

Cell proliferation was studied after incubating cells with the test sample, including control, NPs, SrRNPs, or the same amount of SrR as the test cells. Fluorescent Calcein cell cytotoxicity kit (Molecular Probes, Eugene, OR) was utilized for qualitative analysis of live cells through fluorescence microscopy. Furthermore, MTT assay was evaluated in triplicate for quantitative assessment of cell viability.

Preparation of Photo-Polymerized Hydrogel Encapsulated SrRNPs

A hydrogel solution was synthesized by mixing 0.2 g/mL PEGDA (MW 3400 Da) in sterilized water. A photoinitiator, Irgacure 2959, was then mixed into the above PEGDA mixture and gently stirred to obtain a desired concentration of the mixture. The SrRNPs were added to the PEGDA polymeric hydrogel solution and mixed to obtain the composite mixture. (SrRNPs-H) Rheological studies of the polymeric photo-cross-linked were performed under different UV light irradiation time (0, 50, or 100 s; 365 nm; 10 mW/cm^2), as similarly described previously.[27] The viscoelastic properties (G′ and G") of photo-cross-linked gels were determined with a rheometer (Haake Rheostress 1). Rheological data of mechanical strength (Y-axis) vs. time (X-axis) were presented.

In vitro Release

Drug release from the composite hydrogels (SrR-H), nanocarrier (SrRNPs) or nanocomposite hydrogels (SrRNPs-H) was elucidated with the same amounts of SrR solution, which were placed in separate dialysis bags (MW 3500 Da). According to previously published literature, the effective dosage of SrR was 0.25–0.5 mM.[6] The amount of SrR (0.3 mM) was then picked in the formulations for the release study. Dialysis bags with various formulations were placed in an aqueous solution inside the tubes under constant stirring using a shaker-plate. The test samples were removed at specific time intervals, and the amount of drug released was measured at approximately 320 nm with UV/VIS spectroscopy using a microplate reader.[13] The percentage of drug released from the nanocomposite hydrogel was evaluated in triplicate.

In vivo Study

Male Wistar rats were obtained from BioLASCO (Taipei, Taiwan) and housed under the control and care of the Laboratory Animal Center of Taipei Medical University. The animal studies were approved by the TMU Institute of Animal Care and Use Committee (LAC-2017-0083, LAC-2018-0007, LAC-2019-0216 and LAC-2020-0157) and procedures were compliances with the standard guidelines of the institutional animal care and use committee of LAC-TMU. Spinal fusion was performed on rodent spine for new bone formation, per previous studies.[28] Anesthesia was achieved with an inhalant of Isoflurane (1–4%). Under aseptic conditions, a dorsal incision around the lumbar and sacral pine area was done for all animals. Prepared formulations were administered in different rats, and the dorsal wounds were sutured with 3.0 nylon without tension. All treated animals were sacrificed in the post-operative of 4 weeks and 8 weeks.

A bone graft was implanted after dorsal decortication in the spinal region for bone regeneration. The male Wistar rats were divided into three groups: control (decortication only), group two (decortication followed by local administration of the developed PEGDA hydrogel), and group three (SrRNPs-H) (local administration of SrR at hydrogel concentration of 0.16 mg/mL after decortication). During the experiment, implants at the spinal region were visualized by X-ray. The radiographic X-ray images were quantitatively analyzed by the ImageJ software. The radiographic grayscale ratio of the decorticated site/surrounding tissue was measured by an image analyzing software (ImageJ).

Osteogenesis Evaluation of Biological Responses

Spinal specimens were harvested at 8 weeks after surgery. Micro-computed tomography with radiographic assessment was performed to measure bone density and biological responses after implantation of the developed formulations. Micro-computed data were thresholded, converted into binary images[29] and their grey-level (pixel) were calculated by using ImageJ software. Bodyweight changes in rats were measured to detect any in vivo toxicity following implantation of the test formulations. Biocompatibility was evaluated for any local biological response, such as inflammation after implantation of the test sample. The animals were sacrificed, and their tissues were harvested at 8 weeks after implantation. All tissues were harvested, formalin-fixed, dehydrated, immersed in various ethanol concentrations, and paraffin-embedded in a standard protocol. Retrieved specimens were fixed in buffered formalin (10% v/v), dehydrated by a graded

ethanol series, and embedded in paraffin. The specimens were then sectioned to around 10 μm-thick sections and stained by hematoxylin and eosin (H&E) to visualize nuclei and cytoplasm. Finally, the H&E-stained tissue sections were observed by an optical microscope. Gait analysis is a systematic investigation of treated animal locomotion, improved by instrumentation to measure animal body movements, body mechanics, and the muscles' bioactivity. Therefore, animal motion ability after decortication on the different administered formulations, the gait analysis of treated animals was then estimated through a Footprint Analysis.

Statistical Analysis

Statistical analysis of experimental data (average ± standard deviation) was conducted using GraphPad Prism ver. 7.01 (Graph Pad Software, La Jolla, CA), Student's *t*-test or SigmaPlot 14 (Systat Software, San Jose, CA). Group comparisons were performed by two-way analysis of variance or Student's *t*-test, and differences in results were considered statistically significant at $p < 0.05$.

Results

Characterization and Optimal Formulation of SrRNPs

Figure 1A shows the NPs formulation with different concentrations of GCS, which is directly related to turbidity as a measure of both the density and size of NPs.[30] As depicted in Figure 1B and C, DLS data indicated an increase in particle sizes from nano-size to micro-size with increasing GCS concentration. A previous study showed that medium-sized materials (ca. 300–500 nm) could be suitable for drug delivery.[31] As mentioned previously, the NPs of approximately 300–500 nm could load therapeutic agents for lesion delivery, resulting in a therapeutic effect.[32] Therefore, the "medium GCS group" was optimized for further analysis. In addition,

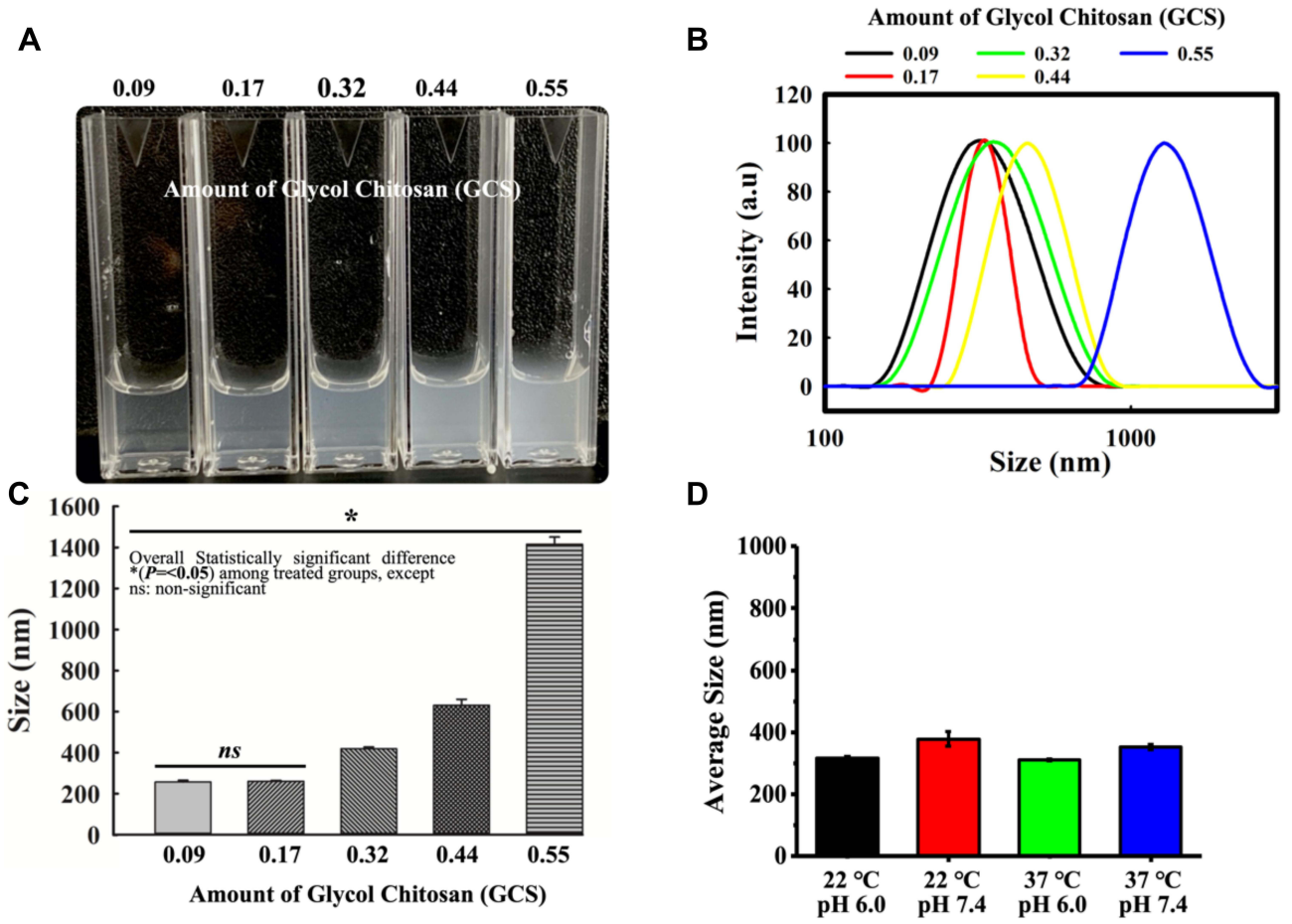

Figure 1 Physicochemical properties and particle size of GCS and HA/SrR-nanocomplex formulation. (**A**) Turbidity development indicating NPs formation with different concentrations of GCS. (**B**) DLS of the particle size distribution for the different formulations (x-axis in log scale). (**C**) Particle sizes of different GCS concentrations (n = 3). (**D**) Average particle sizes of the medium GCS group under different pH and temperature conditions. (n = 3, *Representing $p<0.05$).

the medium GCS group showed pH and temperature stability, DLS data (Figure 1D). Stability enhancement is likely derived from the partial charge donation of anionic HA, thus boosting the durability of SrRNPs during the aqueous phase. This finding was also consistent with a previous finding that polysaccharide-based NPs are resistant to harsh pH environments.[33]

The SrRNPs had negative zeta potential (Figure 2A), as confirmed by DLS analysis. The TEM and SEM micromorphological evaluation revealed that the nanomaterials comprised sphere-shaped NPs of nano-sized distribution (Figure 2B). FTIR data (Figure 2C) showed the spectral analysis that indicated the test sample chemical structure, which revealed chemical changes during the developed formulation fabrication process.

As depicted in Figure 2C, the SrR peak is approximately 1083, and 1317 cm^{-1}.[13] HA, the possible CH_2 with symmetric stretching vibration of approximately 2872 cm^{-1} was found. The peak at around 1033 cm^{-1} with C\O\C hemiacetalic system in both HA and NPs was confirmed.[34] GCS and NPs bands around 3400 to 3200 cm^{-1}, corresponding to NH_2 and OH groups' stretching vibration. Thus, the FTIR analysis could prove the coexistence of NPs in HA, GCS, and SR (Figure 2C).

Cellular Interactions – Proliferation

Figure 3A and B revealed various growth patterns of osteoblasts following incubation with the developed formulations. Cell viability analysis showed that on days 3 and 7, the SrRNPs-treated groups had significant differences in growth patterns compared with the other experimental groups (Figure 3B). Moreover, the SrR-treated group showed significant differences in growth patterns compared with the control group on days 3 and 7 (Figure 3B). Hence, SrRNPs were shown to support osteoblastic cell proliferation.

Figure 3C shows that a weak Cy5-nanocarrier fluorescent signal appeared around the cells, as observed under fluorescent microscopy (pretreatment of HA: I). On the contrary, the group that received SrRNPs without HA pretreatment (II) exhibited elevated accumulation of Cy5-nanocarrier around the cytoplasm of osteoblasts. This result implied that bone cells might express the HA receptor to interact with HA-containing carriers.[35,36]

Cellular Interactions – ARS Findings

As reported earlier, SrR intake-induced elevation of the calcium-sensing receptor's bioactivation could induce genes associated with osteoblastic growth and maturation, and ARS staining can reflect the maturation of osteoblasts.[37–40] In this study, four treatment groups of osteoblast cells (untreated control, SrR-treated cells, NPs only-treated cells, and SrRNPs-treated cells) were subjected to ARS staining for microscopic observation and quantitative measurement. As shown in Figure 4A and B, three groups of cells (control, SrR-treated, and

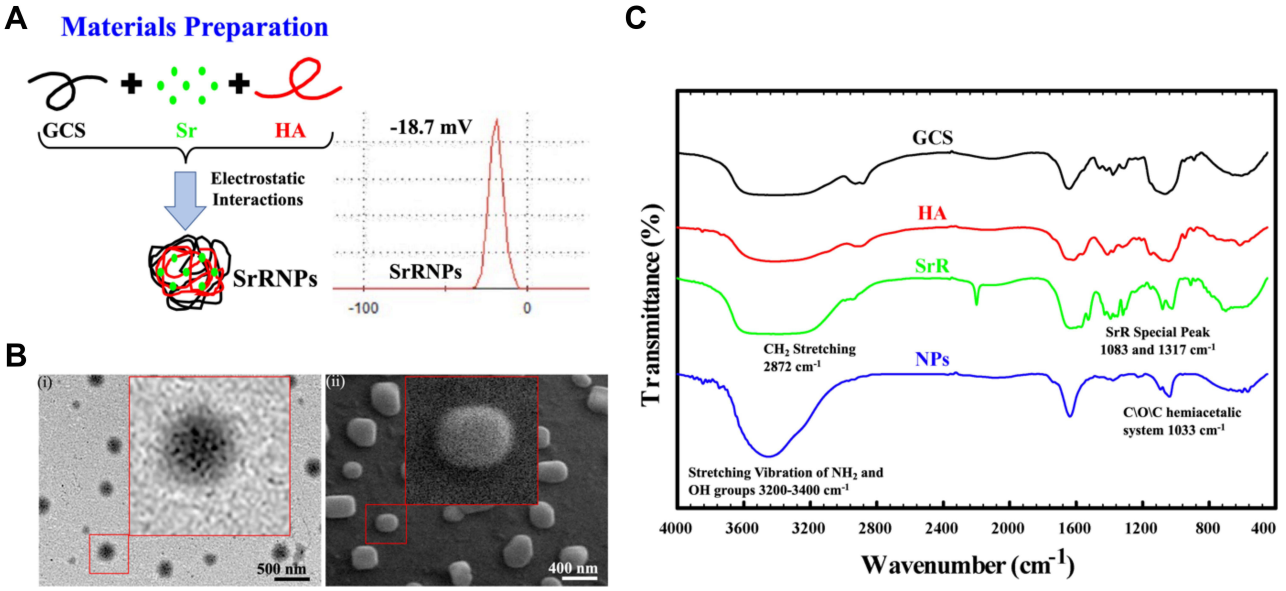

Figure 2 Physicochemical properties. (**A**) Zeta potential of NPs in aqueous dispersions displaying the surface charge distribution on the SrRNPs. (**B**) TEM (i) and SEM (ii) micro-morphological evaluation. (**C**) FTIR spectra of different compounds.

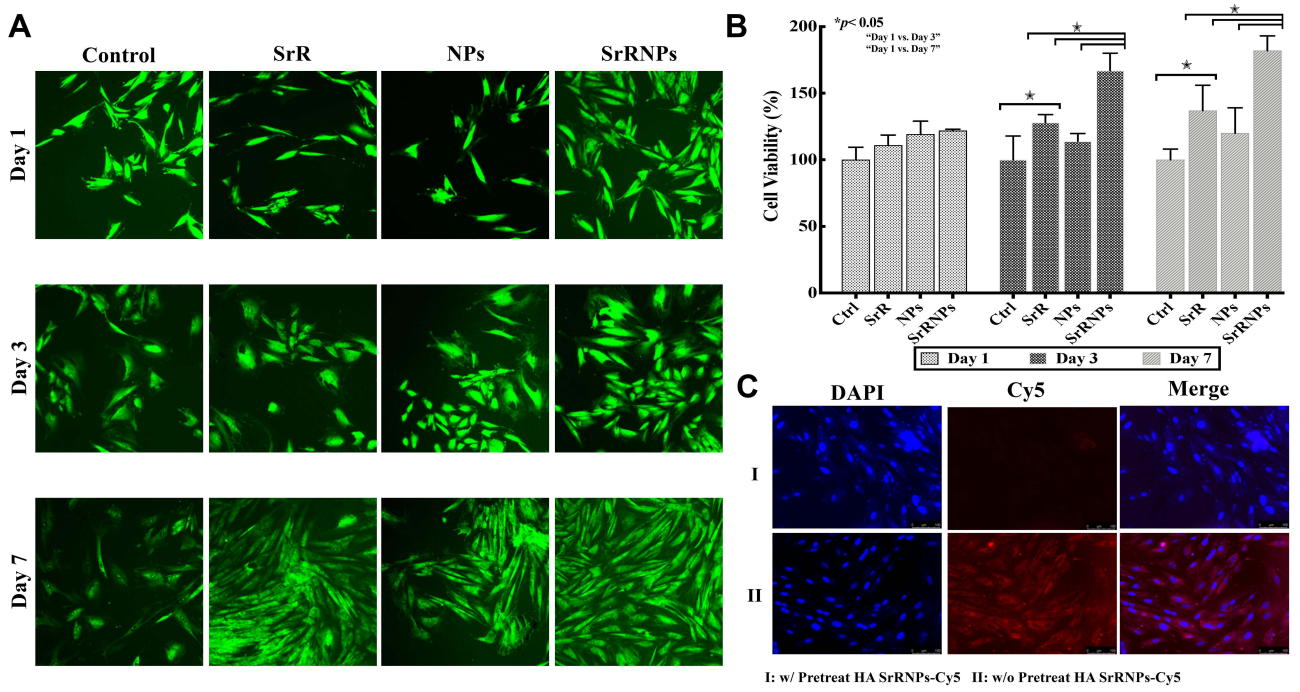

Figure 3 Cellular interactions – proliferation. (**A**) Cell viability assay (Calcein-AM) showing the biological effect of SrR, NPs, and SrRNPs on cells compared with the untreated control group. (**B**) MTT quantitative assay. (**C**) Cellular binding affinity of Cy5-nanocarrier with or without pretreatment with an HA inhibitor, as observed under fluorescent microscopy. (n = 3, *Representing $p<0.05$).

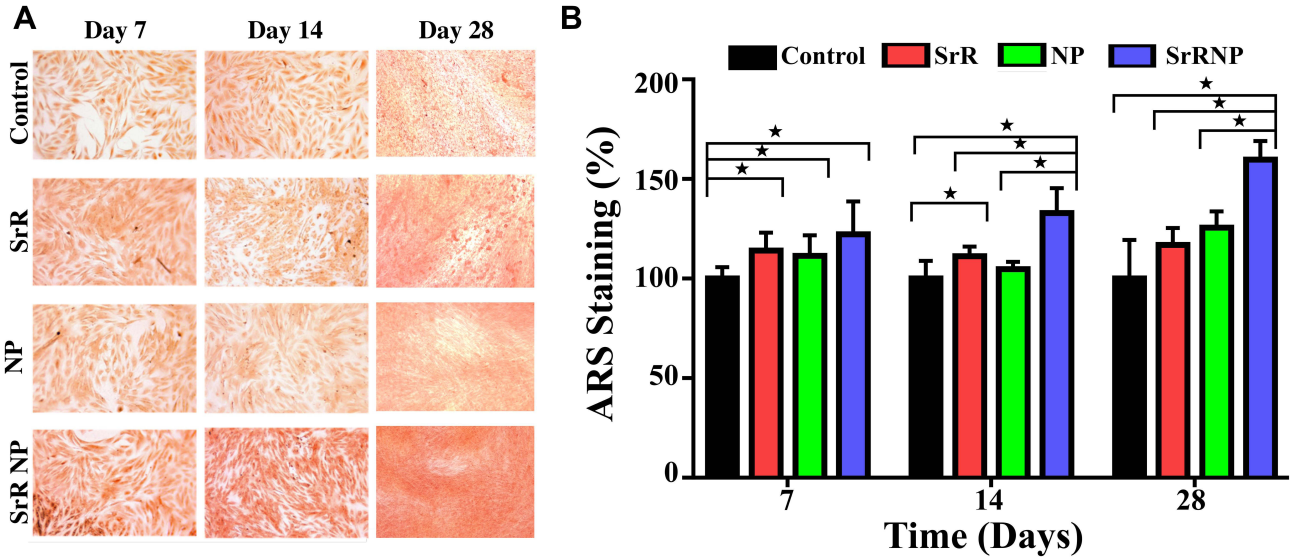

Figure 4 (**A**) ARS staining for the intracellular metal deposition under light microscopy and (**B**) ARS quantitative analysis (OD 405 nm) for different groups on days 7, 14 and 28. (*Representing $p<0.05$).

NPs-treated cells) showed a lower degree of ARS staining (color) than the cells treated with SrRNPs. The reason may be that the cellular uptake of SrRNPs containing HA has potentially increased via HA receptor-mediated endocytosis (Figure 3C). Through effective HA receptor-mediated drug delivery, the SrR in a polymeric encapsulated formulation was effectively taken up into cells (Figure 3C), thus promoting osteoblastic growth and maturation, as detected by ARS staining. However, the NPs did not have an active stimulator for cell growth and, therefore, did not significantly differ compared with the untreated control (day

14 and 28). Although the same amount of SrR was used and some therapeutic effect was observed, free-form SrR lacked target selectivity, which restricted its therapeutic potential and resulted in insufficient drug delivery to osteoblasts.

Characteristics of Polymeric Hydrogels

The gel-tunable mechanical behavior of these materials under constant UV light intensity is shown in Figure 5A; the rheological property changed with increasing or decreasing UV-irradiation time. The rheological test results indicated that the polymeric hydrogels' rigidity increased as UV exposure time increased. As shown in Figure 5B, once the hydrogels were incorporated in SrRNPs (SrRNP-H group), macromolecules, or small molecular, SrR was slowly released via the embedded nanocarrier and hydrogel (H), compared with the groups of free-form SrR, SrRNP and SrR-H. The diffusion through the hydrogel meshes without burst release could preserve the local therapeutic level of SrRNPs over time to reduce the risk of unwanted adverse effects and pain.[41]

SEM morphological analysis of the synthesized hydrogels showed porous microstructures, a necessary standard for tissue-engineered scaffolds appropriate for bone regeneration (Figure 5C). The anti-gravity experiment was aimed to evaluate the maintenance of the structural integrity, gel property, and durability of the developed hydrogels. The results showed that the PEGDA polymeric-based solution without UV irradiation was dropped onto the bottom of a test vial due to the lack of adequate mechanical strength. However, exposure of the PEGDA constructed solution to UV irradiation (for 100 s) resulted in a strong gel formation, which remained stable up to 8 weeks (Figure 5D). This result approached the standard criterion for designing ideal bio-hydrogels to be used in future bone tissue engineering applications, per previous studies.[27]

In vivo Study

The evaluation of the implanted test samples and bone regeneration efficiency was carried out after decortication surgery and implantation of various test formulations (8

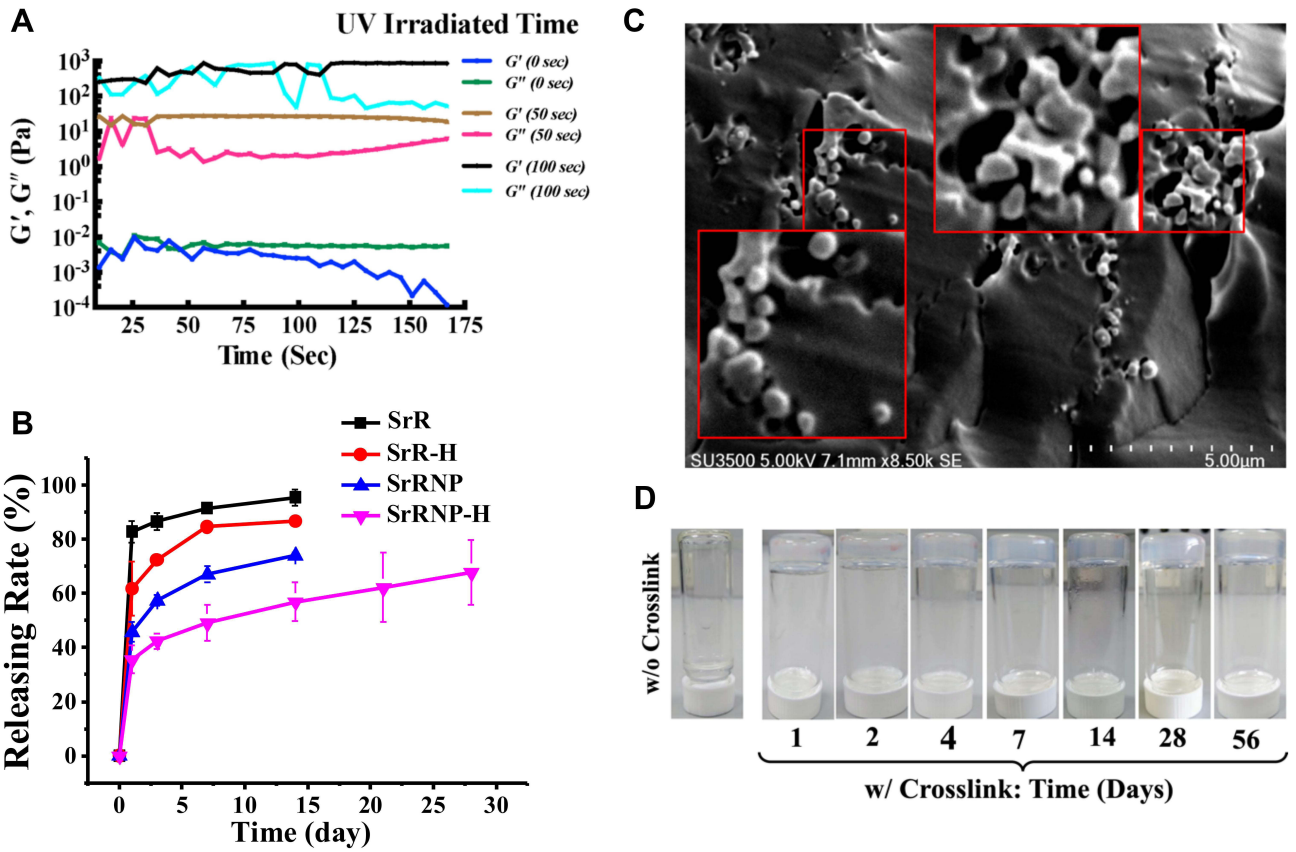

Figure 5 Physio-mechanical property of various test formulations. (**A**) Rheological study under different UV irradiation times. (**B**) In vitro release rate of SrR from different test formulations (n = 3). (**C**) SEM micro-morphological images of the SrRNPs-H. (**D**) Anti-gravity experimental imaged for up to 56 days.

weeks). The X-ray revealed new bone formation with a high radiographic gray level in the SrRNPs-H group (Figure 6A and B). The micro-3D CT images also indicate new bone formation in the surgical site (compact bone structure and higher bone density) in the SrRNPs-H group, as shown in Figure 6C. A significant increase in grey level of thresholded CT binary image was observed in the SrRNPs-H group compared with only decortication and decortication with hydrogel groups, suggesting the process of new bone tissue formation (Figure 6C).

The tissue histopathological evaluation by H&E staining reveals the purple-stained region indicating the progress of possible new bone tissue formation (possibly hydroxyapatite carrier particles). Thus, revealing that the SrRNPs-H group had good healing and active bone regeneration (Figure 7A). Histological evaluation of other organs was conducted to detect any potential in vivo toxic responses, particularly in the kidneys and liver.[42] The results showed no histopathological abnormalities in the liver and kidney. The kidney and liver for both groups receiving decortication with PEGDA hydrogel (H) or SrRNPs-H show no apparent changes, compared with decorticated only (control) (Figure 7B). Thus, implying that the results of the designed formulation exerted no in vivo toxicity effect after implantation. The gait analysis shows that the group that received decortication and SrRNPs-H has a similar strider time ratio/duty factor with the normal control group, while higher than the group receiving only decortication or decortication w/H (Figure 7C). The footprint imaged through gait analysis for the animal given SrRNPs-H was dynamically estimated and recorded (Figure 7D). From the previous study,[43,44] stride behavior is associated with the affected limb pathology. In normal health condition, the stride time ratio between hind and fore is similar, whereas the incomplete therapeutic treatment of test animal (decortication alone or decortication plus H group) causing painful symptom might result in the imbalance stride time ratio and duty factor. The gait data suggested that SrRNPs-H treated group has a similar stride time ratio with duty factor as normal health group, compared to other treated groups (decortication and decortication w/H), implying an improved therapeutic efficacy.

Discussion

Carrier-based site-specific drug delivery systems reduce drug side effects and loss during therapeutic procedures. The selection of suitable drug carriers and active drug components is crucial, affecting drug release behavior. Nano-drug carrier systems can prolong the release of an active drug, thereby improving its pharmacological activity.[45] Thus, polymeric NPs can be significant drug carriers to deliver specific medication to a site-specific on the body. Recently, polymeric NPs have emerged as a promising strategy to achieve desired drug release profiles and therapeutic outcomes. Nano-encapsulation is a modern drug encapsulation method that allows efficient loading of drug molecules inside NPs.[46] This approach may reduce the undesirable effects associated with drugs. Key factors in designing polymeric NPs for drug encapsulation are polymer selection, polymeric concentration, drug and polymer ratio, and the nature and amount of drugs suitable for drug delivery with NPs. This research focused on developing modern nanoparticle system with osteogenetic medication to improved bone healing.

GCS and HA are functional biomaterials widely used for the delivery of various types of drug formulations. Both materials are inexpensive and can be used as suitable excipients in numerous pharmaceutical formulations along with active drug substances.[47,48] Sr^{2+}, as an active drug, can stimulate osteogenesis, thus promoting the cellular proliferation and differentiation of osteoblasts and resulting in new bone formation. As a stimulant, Sr^{2+} promotes bone cell differentiation and migration through potential calcium-sensing receptor pathways, resulting in osteoblast proliferation.[49] In this study, SrR, as an active drug, was encapsulated in NPs containing different amounts of GCS with HA, formulated based on electrostatic interaction in a weakly acidic pH environment.

Regarding polymer GCS concentration effect on particle size, it is known that the particle size of the nanoparticles increased with increasing polymer chitosan concentrations in all cases, confirming the previous publications.[50,51] An increase in polymer solution internal phase viscosity could increase particle size. Particle size reduction could be caused by the impact that the viscosity of the internal phase of the polymeric emulsion might be changed based on the polymeric type used too.[52] Medium size nanoparticles (300–500 micrometer) should be suitable for local drug delivery. From Figure 1, we can find that our medium size GCS HA nanoparticles are stable at room and body temperature. Besides, these nanoparticles are stable in different pH levels. The following in vitro and in vivo studies also revealed our SrRNP treated group can have good osteogenesis effect. Encapsulation efficiency increases with increasing chitosan polymer concentration.[53] HA is found abundantly as an

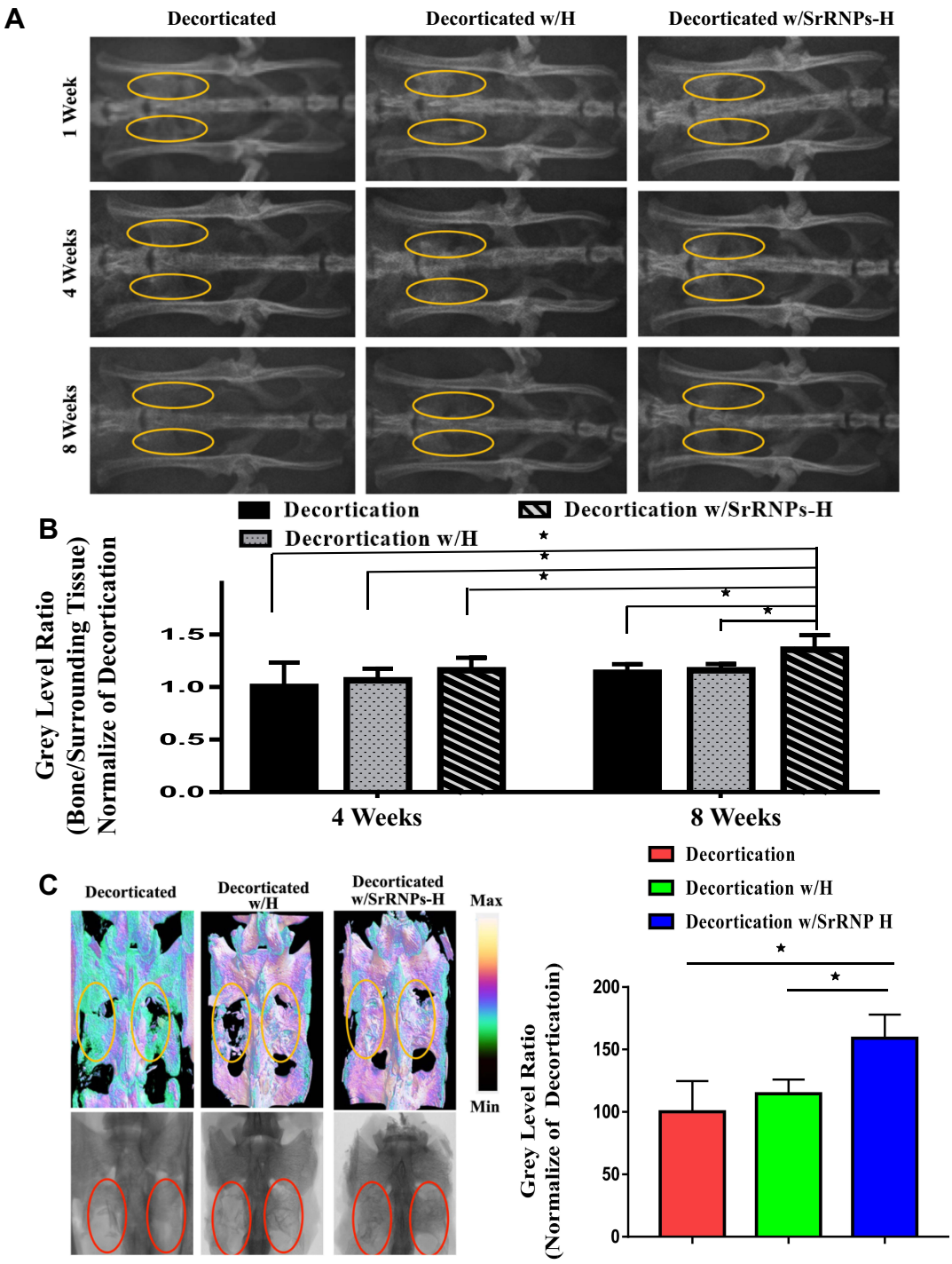

Figure 6 In vivo bone regeneration efficacy evaluation. (**A**) X-ray evaluation after 1, 4, and 8 weeks. (**B**) Gray-level evaluation by ImageJ software for X-ray in the treated groups. (**C**) Micro-CT in vivo imaging analysis after scarification and grey level of thresholded binary CT image evaluation by ImageJ software in different groups (n = 6, *Representing $p<0.05$).

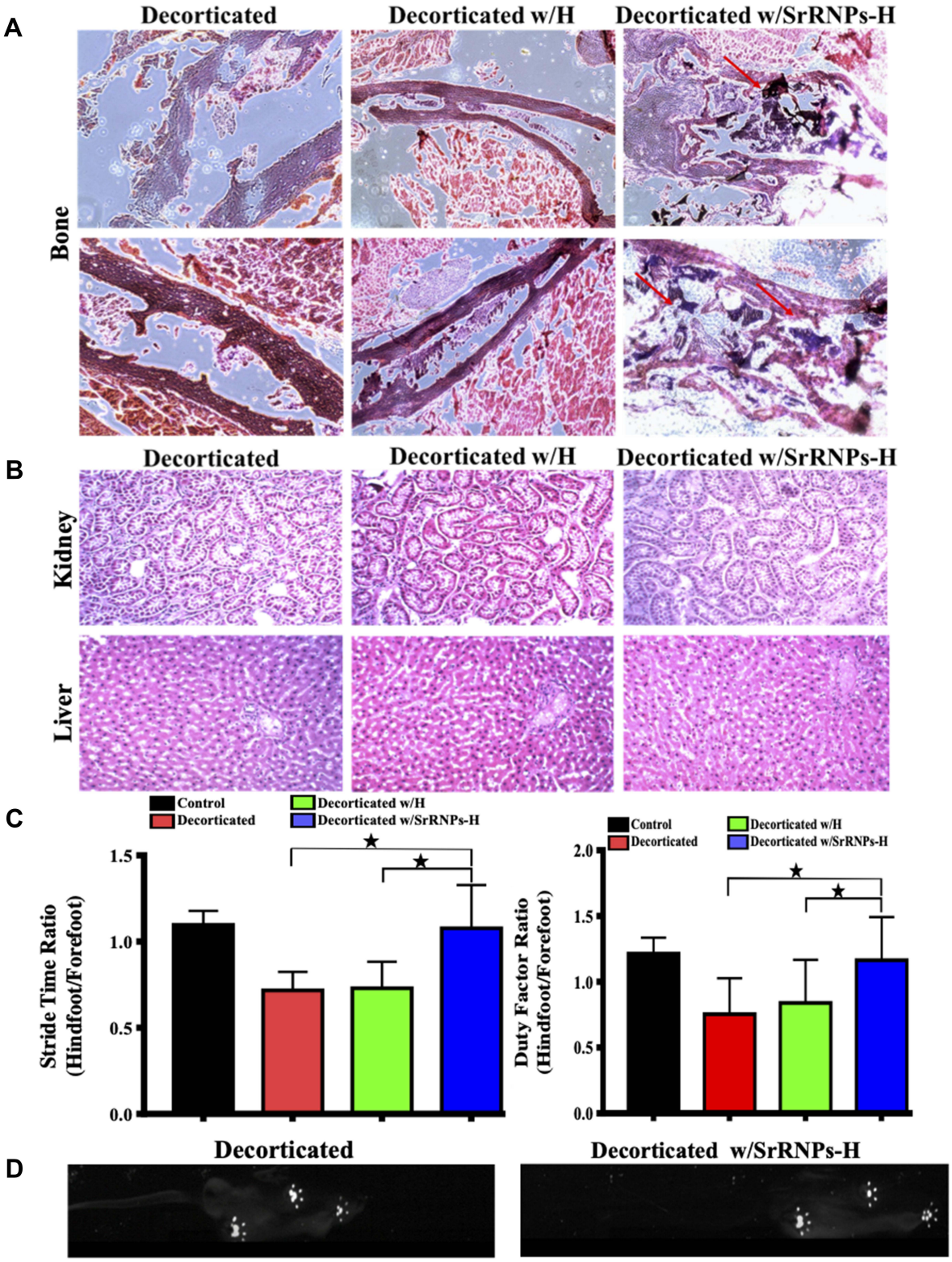

Figure 7 In vivo bone regeneration mechanism. (**A**) Histologic analysis of the spinal region treated with various formulations. (**B**) In vivo toxicity evaluation for soft tissues with H&E staining. The test animal gait analysis: (**C**) quantitatively, and (**D**) qualitatively (Decortication and Decortication w/SrRNPs-H). (n=6, *Representing $p<0.05$).

integral part of all bones and cartilage throughout the body. Over the years, HA polymer and its nanoformulation have received growing attention for bone tissue engineering and orthopedic application due to their superior biocompatibility and unique wide range of drug encapsulation properties. The surficial charge of polymeric NPs is an important feature affecting the tissue distribution profiles and toxicity of encapsulated drug molecules. Typically, anionic nanomaterials are much safer than cationic nanomaterials,[54] with several advantages over the latter.[55] Our SrRNP revealed −18.7 mV in DLS examination. The safety of SrNPH could also be confirmed by the in vivo and in vitro examination.

Chitosan, collagen/gelatin, alginate, silk, peptides, and HA are naturally derived polymeric biomaterials widely used for bone tissue engineering.[56] During bone development, growth, remodeling, osteocytes, and osteoblasts express specific HA receptors (such as CD44).[36] Furthermore, the CD44 ectodomain contains an HA-binding motif for proteoglycans and other proteins binding.[57] Polymeric nanocarrier drug delivery systems containing HA can promote possible HA receptor-mediated cellular interactions. An inhibition study can further be conducted, in which an HA-containing medium is pretreated to uphold the active position of the HA receptor. In Figure 3C, we can find that the fluorescent SrRNP can enter cell to show cy5 fluorescence in the cytoplasm without pretreat HA. This result could suggest that HA receptor could help nanoparticle to enter cell.

The prepared anionic nanoformulation (SrRNPs) exhibited low cytotoxicity, a tendency to accumulate in osteoblasts, and good osteogenesis ability (Figure 4). Nonetheless, the effect of SrRNPs on osteoblastic cellular growth needs to be improved via a 3D structural scaffold for attachment, proliferation, migration, and angiogenesis for nutrients and wastes transport during bone regeneration. Polymeric material could be an appropriate biomaterial-scaffold for drug delivery in biomedical tissue engineering owing to their unique tunable mechanical features. It can also encapsulate active pharmaceutical ingredients such as SrR and act as a relevant multiple drug carrier system. More interestingly, it can mimic the extracellular matrix at specific tissue sites. Additional benefits include their ability to prolong the release of encapsulated drugs, which results in the maintenance of high therapeutic concentration of the drug over a long period. The synthesized biomaterial-scaffold also had the appropriate physicochemical properties for maintaining the local therapeutic concentration of active SrR nanoformulation. Photopolymerized hydrogels, such as PEGDA, have also been used as a fascinating local drug delivery system[58] and controlled drug release system.[59] Once hydrogels were incorporated with SrRNPs, small molecular medicines (SrRs) are released via diffusion of the network, thus preserving high local concentrations of medicines for a long time, which could reduce the risk of side effects and patient discomfort.[41] Recently, photopolymerized hydrogels are appealing for the local delivery of medicines. According to previous research, 100 s of UV exposure can produce the appropriate hydrogels for spinal fusion. This UV treatment has been considered an appropriate hydrogel fabrication method for incorporating biologically active ingredients that can be applied in vivo.[27] Figure 5, which details the mechanical strength with drug release profiles of the test formulations. Only SrR was released rapidly from the dialysis bag without hindrance. However, SrR encapsulated in PEGDA hydrogels was released faster than SrRNP group or the group of SrRNP embedded within PEGDA (SrRNPs-H). The possible reason is that the release of the free-form of SrR encountered fewer barriers than SrRNPs firmly encapsulated within the hydrogel. Further, the controlled diffusion process profoundly impacts the sustained release of drug/nanomedicine from the developed hydrogels.[60] The crosslinked networks surrounding the hydrogel encapsulating the drug were an additional diffusion barrier responsible for slowing down the drug release rate (Figure 5B).

According to an earlier publication,[61] controlled, sustained drug delivery to targeted organs offers adequate local therapeutic (effective) windows and reduces the systemic drug exposure. This strategy decreases the adverse effects of drug released into the systemic circulation. In this study, drug-loaded hydrogels were spread in a dialysis bag to mimic local administration.

In the in vitro analysis, SrR release studies indicated that SrRNPs-H sustainably and steadily released 60–70% of the encapsulated SrR for up to 4 weeks compared with free-from SrR and SrR-H (to reach a plateau after day 7). As mentioned previously, Canalis et al stated that 0.01 mM SrR increases bone formation in rodent cells, and additional investigation indicated a meaningful increase in osteogenic biomarkers in human mesenchymal stem cells (MSCs) treated with 0.024–0.24 mM SrR.[62,63]

It is reasonable that the continuous and steady release rate of SrR in the SrRNPs-H group exceeded the effective dosage within 10 days, consistent with a previous finding.[64] The slow release of SrR, as shown in the

SrRNPs-H group, could enhance its therapeutic effect on bone regeneration. In any case, SrR release from the SrRNPs-H group was slower than from SrR-H or SrRNP group, indicating that the multiple encapsulation system had more firmly preserved the encapsulated SrR in environmental conditions that favor drug release. Further, indicate that the SrRNPs-H could maintain the entrapped SrR in lesion, preventing its uncontrolled biodistribution within the body circulation. SrR can be released at a high activity level in bone defects. Moreover, the SrR release slowdown from SrRNPs-H could improve and prolong the drug's therapeutic efficacy by enabling a continuous release of the encapsulated SrR in bone defect. This strategy could be an optimal approach to provide effective drug concentrations to cells.[65]

Besides, drugs' therapeutic effects are usually restricted by their inability to sustain their therapeutic levels at the lesion site.[66] Thus, drug formulations with sustained drug release kinetics often show a slow therapeutic bioactivity duration compared with those with rapid drug release kinetics. Formulations with targeted or sustainable drug release could lead to extensive exposure of the lesion to high concentrations of drugs, thereby preventing the inconvenience of continuous therapeutic level maintenance and diminishing the unwanted toxic side effects of drugs. Local administration enables low drug uptake by systemic cells.[67] The therapeutic effect and safety of SrRNP-H in vivo can be proved by our histological, radiographic and gait walkability analysis in Figures 6 and 7. The kidney and liver slices in three groups revealed the same cell microstructures without obvious differences. A constant dosage of drugs within the therapeutic window is also important and helpful for treatment.[68]

As reported previously, new bone formation begins from local hematoma with enriched cytokines, which augment the permeability of vessel and chemotaxis effect. Once the MSCs migrate into the hematoma site, they begin to proliferate and differentiate into osteoblasts. These new progenitor cells would lay down osteoid or ECM and transfer it to bone through mineralization.[69] As more and more mineralization in bone tissue, the inorganic section of bone gradually increases. Hydroxyapatite substances take 60–70% of all inorganic section of bone. Thus, hydroxyapatite could present very light purple around the new bone site's formation in the H&E stain. Once the bone becomes mature, hydroxyapatite developed dark purple in H&E stain.[70,71] Thus, active osteoblasts could produce irregular crystals of hydroxyapatite, as shown in the in vivo data suggesting the identified new bone formation site from the SrRNPs-H treated group through microscopic histological analysis.

Bone fusion is a standard orthopedic surgical procedure for reconstruction in traumatic and degenerative joint deformities. Studies in animal models also showed that bone fusion procedures, such as spinal fusion and joint fusion, are safe, effective, and cheap treatment strategies with low complications.[72] The therapeutic effect of local administration with SrRNPs-H on new bone regeneration was found in a bone decortication rat model. From Figure 6, we can see that more bone formation in the SrRNP-H group under CT and X-ray image. The quantitative evaluation of X-ray and CT also revealed a significance difference compared to other group (8 weeks).

The gait analysis can be the useful tool to evaluate postoperative animal motion. The temporospatial characteristics of animal gaits could be recorded in detail. There are several studies focus on rodent gait analysis in the literature, however, few studies of them mentioned about the gait change after spinal fusion. Many factors including age, body weight, species and gender can affect parameters of gait analysis.[73,74] We selected ratio of stride time of forefoot and hindfoot for experiment. The duty factor is defined as the ratio between stance time and stride time. We could find that the data of duty factor ratio were decreased in decortication and decortication-H treated group. The data of stride time ratio also were decreased in decortication and decortication-H treated group. The results could be because the rats had painful hindfoot with poor bone healing results. The overall gait data should support our radiographic and histological examinations that the SrRNP-H treated group has a promising osteogenesis effect on bone healing.

Conclusions

In this study, unique composite hydrogels (SrRNPs-H) were developed for the first time. Further, their biocompatibility and efficacy were successfully evaluated in a bone decortication rat model. Our results suggested that the group treated with SrRNPs-H had a higher degree of bone regeneration than the other groups. The successful developed therapeutic approach could be highly afforded with biocompatibility, sustained drug release, possible HA receptor-mediated cellular interaction. More interestingly, the hydrogel carrier promoted local site-effective delivery of SrR, as illustrated in Figure 8. Thus, owing to its multiple unique functionalities, the SrR polymer composite hydrogel

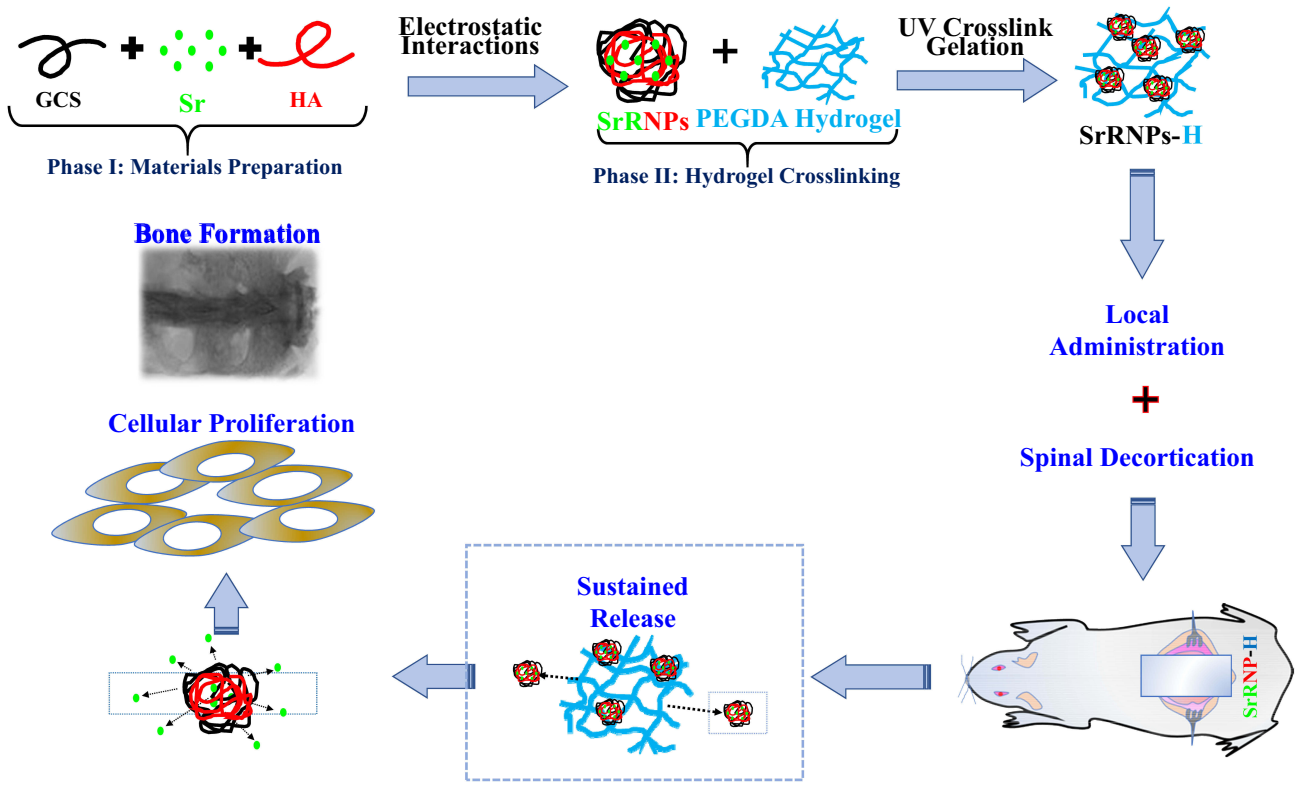

Figure 8 The schematic illustration of this research.

formulation may be a novel potential alternative to oral SrR in future orthopedic clinical applications.

Acknowledgments

This original paper was supported by a government project from the Ministry of Science and Technology (MOST), Taiwan (MOST 108-2221-E-038-017-MY3; MOST 108-2320-B-038-061-MY3). Chih-Wei Chiang and Chih-Hwa Chen are the first two co-authors and made equal contributions.

Disclosure

The authors report no conflicts of interest for this work.

References

1. Boucher HH. A method of spinal fusion. *J Bone Joint Surg Br*. 1959;41-B(2):248–259. doi:10.1302/0301-620X.41B2.248
2. Papa S, Vismara I, Mariani A, et al. Mesenchymal stem cells encapsulated into biomimetic hydrogel scaffold gradually release CCL2 chemokine in situ preserving cytoarchitecture and promoting functional recovery in spinal cord injury. *J Control Release*. 2018;278:49–56. doi:10.1016/j.jconrel.2018.03.034
3. Tuchman A, Brodke DS, Youssef JA, et al. Iliac crest bone graft versus local autograft or allograft for lumbar spinal fusion: a systematic review. *Global Spine J*. 2016;6(6):592–606. doi:10.1055/s-0035-1570749
4. Mobasheri A. The future of osteoarthritis therapeutics: targeted pharmacological therapy. *Curr Rheumatol Rep*. 2013;15(10):364. doi:10.1007/s11926-013-0364-9
5. Tsai TT, Tai CL, Ho NY, et al. Effects of strontium ranelate on spinal interbody fusion surgery in an osteoporotic rat model. *PLoS One*. 2017;12(1):e0167296. doi:10.1371/journal.pone.0167296
6. Guo X, Wei S, Lu M, et al. Dose-dependent effects of strontium ranelate on ovariectomy rat bone marrow mesenchymal stem cells and human umbilical vein endothelial cells. *Int J Biol Sci*. 2016;12(12):1511–1522. doi:10.7150/ijbs.16499
7. Cianferotti L, D'Asta F, Brandi ML. A review on strontium ranelate long-term antifracture efficacy in the treatment of postmenopausal osteoporosis. *Ther Adv Musculoskelet Dis*. 2013;5(3):127–139. doi:10.1177/1759720X13483187
8. Langdahl BL. Oxford Desk Reference Endocrinology. In: Turner HE, Eastell R, Grossman A, editors. *Oxford Desk Reference Endocrinology*. Oxford University Press; 2018:342–346.
9. Tian A, Zhai JJ, Peng Y, et al. Osteoblast response to titanium surfaces coated with strontium ranelate-loaded chitosan film. *Int J Oral Maxillofac Implants*. 2014;29(6):1446–1453. doi:10.11607/jomi.3806
10. Nair BP, Sindhu M, Nair PD. Polycaprolactone-laponite composite scaffold releasing strontium ranelate for bone tissue engineering applications. *Colloids Surf B Biointerfaces*. 2016;143:423–430. doi:10.1016/j.colsurfb.2016.03.033
11. Tsolaki IN, Madianos PN, Vrotsos JA. Outcomes of dental implants in osteoporotic patients. A literature review. *J Prosthodont*. 2009;18(4):309–323. doi:10.1111/j.1532-849X.2008.00433.x
12. Zhou D, Qi C, Chen YX, et al. Comparative study of porous hydroxyapatite/chitosan and whitlockite/chitosan scaffolds for bone regeneration in calvarial defects. *Int J Nanomedicine*. 2017;12:2673–2687. doi:10.2147/IJN.S131251

13. Deepthi S, Abdul Gafoor AA, Sivashanmugam A, Nair SV, Jayakumar R. Nanostrontium ranelate incorporated injectable hydrogel enhanced matrix production supporting chondrogenesis in vitro. *J Mater Chem B*. 2016;4(23):4092–4103. doi:10.1039/C6TB00684A
14. Yang Y, Zhao Y, Lan J, et al. Reduction-sensitive CD44 receptor-targeted hyaluronic acid derivative micelles for doxorubicin delivery. *Int J Nanomedicine*. 2018;13:4361–4378. doi:10.2147/IJN.S165359
15. Jia X, Han Y, Pei M, et al. Multi-functionalized hyaluronic acid nanogels crosslinked with carbon dots as dual receptor-mediated targeting tumor theranostics. *Carbohydr Polym*. 2016;152:391–397. doi:10.1016/j.carbpol.2016.06.109
16. Liao J, Zheng H, Hu R, et al. Hyaluronan based tumor-targeting and pH-responsive shell cross-linkable nanoparticles for the controlled release of doxorubicin. *J Biomed Nanotechnol*. 2018;14(3):496–509. doi:10.1166/jbn.2018.2510
17. Felszeghy S, Modis L, Tammi M, Tammi R. The distribution pattern of the hyaluronan receptor CD44 during human tooth development. *Arch Oral Biol*. 2001;46(10):939–945. doi:10.1016/S0003-9969(01)00053-X
18. Tomar L, Tyagi C, Kumar M, et al. In vivo evaluation of a conjugated poly(lactide-ethylene glycol) nanoparticle depot formulation for prolonged insulin delivery in the diabetic rabbit model. *Int J Nanomedicine*. 2013;8:505–520. doi:10.2147/IJN.S38011
19. Xue P, Zhang XY, Chuah YJ, Wu YF, Kang YJ. Flexible PEGDA-based microneedle patches with detachable PVP-CD arrowheads for transdermal drug delivery. *Rsc Adv*. 2015;5(92):75204–75209. doi:10.1039/C5RA09329E
20. Seo J, Lee J, Na K. Polymeric materials for drug release system in drug eluting stents. *J Pharm Investig*. 2016;46(4):317–324. doi:10.1007/s40005-016-0251-2
21. Zarins J, Pilmane M, Sidhoma E, Salma I. Does local application of strontium increase osteogenesis and biomaterial osteointegration in osteoporotic and other bone tissue conditions: review of literature. *Acta Chir Latv*. 2016;16(2):17. doi:10.1515/chilat-2017-0004
22. Eskandar NG, Simovic S, Prestidge CA. Chemical stability and phase distribution of all-trans-retinol in nanoparticle-coated emulsions. *Int J Pharm*. 2009;376(1–2):186–194. doi:10.1016/j.ijpharm.2009.04.036
23. Li Y, Pan S, Zhang W, Du Z. Novel thermo-sensitive core-shell nanoparticles for targeted paclitaxel delivery. *Nanotechnology*. 2009;20(6):065104. doi:10.1088/0957-4484/20/6/065104
24. Huang YC, Li RY. Preparation and characterization of antioxidant nanoparticles composed of chitosan and fucoidan for antibiotics delivery. *Mar Drugs*. 2014;12(8):4379–4398. doi:10.3390/md12084379
25. Frosch KH, Sondergeld I, Dresing K, et al. Autologous osteoblasts enhance osseointegration of porous titanium implants. *J Orthop Res*. 2003;21(2):213–223. doi:10.1016/S0736-0266(02)00143-2
26. Key J, Dhawan D, Cooper CL, et al. Multicomponent, peptide-targeted glycol chitosan nanoparticles containing ferrimagnetic iron oxide nanocubes for bladder cancer multimodal imaging. *Int J Nanomedicine*. 2016;11:4141–4155. doi:10.2147/IJN.S109494
27. Chiang CW, Chen WC, Liu HW, Wang IC, Chen CH. Evaluating osteogenic potential of ligamentum flavum cells cultivated in photo-responsive hydrogel that incorporates bone morphogenetic protein-2 for spinal fusion. *Int J Mol Sci*. 2015;16(10):23318–23336. doi:10.3390/ijms161023318
28. Zwolak P, Farei-Campagna J, Jentzsch T, von Rechenberg B, Werner CM. Local effect of zoledronic acid on new bone formation in posterolateral spinal fusion with demineralized bone matrix in a murine model. *Arch Orthop Trauma Surg*. 2018;138(1):13–18. doi:10.1007/s00402-017-2818-4
29. Panmekiate S, Ngonphloy N, Charoenkarn T, Faruangsaeng T, Pauwels R. Comparison of mandibular bone microarchitecture between micro-CT and CBCT images. *Dentomaxillofac Radiol*. 2015;44(5):20140322. doi:10.1259/dmfr.20140322
30. Miller VM, Hunter LW, Chu K, et al. Biologic nanoparticles and platelet reactivity. *Nanomedicine*. 2009;4(7):725–733. doi:10.2217/nnm.09.61
31. Zariwala MG, Elsaid N, Jackson TL, et al. A novel approach to oral iron delivery using ferrous sulphate loaded solid lipid nanoparticles. *Int J Pharm*. 2013;456(2):400–407. doi:10.1016/j.ijpharm.2013.08.070
32. O'Neill CP, Dwyer RM. Nanoparticle-based delivery of tumor suppressor microRNA for cancer therapy. *Cells*. 2020;9(2):521. doi:10.3390/cells9020521
33. Barbosa AI, Costa Lima SA, Reis S. Application of pH-responsive fucoidan/chitosan nanoparticles to improve oral quercetin delivery. *Molecules*. 2019;24(2):346. doi:10.3390/molecules24020346
34. Vasi AM, Popa MI, Butnaru M, Dodi G, Verestiuc L. Chemical functionalization of hyaluronic acid for drug delivery applications. *Mater Sci Eng C Mater Biol Appl*. 2014;38:177–185. doi:10.1016/j.msec.2014.01.052
35. Ou C-Y, Chang N-K, Lee T-H, et al. Obtainment of mesenchymal stem cells by surgeons. *Formos J Surg*. 2014;47(4):166–170. doi:10.1016/j.fjs.2014.04.002
36. Li Y, Zhong G, Sun W, et al. CD44 deficiency inhibits unloading-induced cortical bone loss through downregulation of osteoclast activity. *Sci Rep*. 2015;5:16124. doi:10.1038/srep16124
37. Caverzasio J. Strontium ranelate promotes osteoblastic cell replication through at least two different mechanisms. *Bone*. 2008;42(6):1131–1136. doi:10.1016/j.bone.2008.02.010
38. Chattopadhyay N, Quinn SJ, Kifor O, Ye C, Brown EM. The calcium-sensing receptor (CaR) is involved in strontium ranelate-induced osteoblast proliferation. *Biochem Pharmacol*. 2007;74(3):438–447. doi:10.1016/j.bcp.2007.04.020
39. Choudhary S, Halbout P, Alander C, Raisz L, Pilbeam C. Strontium ranelate promotes osteoblastic differentiation and mineralization of murine bone marrow stromal cells: involvement of prostaglandins. *J Bone Miner Res*. 2007;22(7):1002–1010. doi:10.1359/jbmr.070321
40. Zhu LL, Zaidi S, Peng Y, et al. Induction of a program gene expression during osteoblast differentiation with strontium ranelate. *Biochem Biophys Res Commun*. 2007;355(2):307–311. doi:10.1016/j.bbrc.2007.01.120
41. Zhao J, Liang X, Cao H, Tan T. Preparation of injectable hydrogel with near-infrared light response and photo-controlled drug release. *Bioresour Bioprocess*. 2020;7(1):1–13. doi:10.1186/s40643-019-0289-x
42. Alsalahi A, Abdulla MA, Al-Mamary M, et al. Toxicological features of catha edulis (khat) on livers and kidneys of male and female sprague-dawley rats: a Subchronic Study. *Evid Based Complement Alternat Med*. 2012;2012:829401. doi:10.1155/2012/829401
43. Lakes EH, Allen KD. Gait analysis methods for rodent models of arthritic disorders: reviews and recommendations. *Osteoarthritis Cartilage*. 2016;24(11):1837–1849. doi:10.1016/j.joca.2016.03.008
44. Herbin M, Hackert R, Gasc JP, Renous S. Gait parameters of treadmill versus overground locomotion in mouse. *Behav Brain Res*. 2007;181(2):173–179. doi:10.1016/j.bbr.2007.04.001
45. Yoo HS, Oh JE, Lee KH, Park TG. Biodegradable nanoparticles containing doxorubicin-PLGA conjugate for sustained release. *Pharm Res*. 1999;16(7):1114–1118. doi:10.1023/A:1018908421434
46. Katouzian I, Jafari SM. Nano-encapsulation as a promising approach for targeted delivery and controlled release of vitamins. *Trends Food Sci Technol*. 2016;53:34–48. doi:10.1016/j.tifs.2016.05.002
47. Choi KY, Chung H, Min KH, et al. Self-assembled hyaluronic acid nanoparticles for active tumor targeting. *Biomaterials*. 2010;31(1):106–114. doi:10.1016/j.biomaterials.2009.09.030
48. Kim JH, Kim YS, Park K, et al. Antitumor efficacy of cisplatin-loaded glycol chitosan nanoparticles in tumor-bearing mice. *J Control Release*. 2008;127(1):41–49. doi:10.1016/j.jconrel.2007.12.014

49. Fromigue O, Hay E, Barbara A, et al. Calcium sensing receptor-dependent and receptor-independent activation of osteoblast replication and survival by strontium ranelate. *J Cell Mol Med*. 2009;13(8B):2189–2199. doi:10.1111/j.1582-4934.2008.00673.x
50. Sreekumar S, Goycoolea FM, Moerschbacher BM, Rivera-Rodriguez GR. Parameters influencing the size of chitosan-TPP nano- and microparticles. *Sci Rep*. 2018;8(1):4695. doi:10.1038/s41598-018-23064-4
51. Omar Zaki SS, Ibrahim MN, Katas H. Particle size affects concentration-dependent cytotoxicity of chitosan nanoparticles towards mouse hematopoietic stem cells. *J Nanotechnol*. 2015;2015:1–5. doi:10.1155/2015/919658
52. Wagh VD, Apar DU. Cyclosporine A loaded PLGA nanoparticles for dry eye disease: in vitro characterization studies. *J Nanotechnol*. 2014;2014:1–10. doi:10.1155/2014/683153
53. Dhakar RC. From formulation variables to drug entrapment efficiency of microspheres: a technical review. *J Drug Deliv Ther*. 2012;2(6).
54. Sharifi S, Behzadi S, Laurent S, Forrest ML, Stroeve P, Mahmoudi M. Toxicity of nanomaterials. *Chem Soc Rev*. 2012;41(6):2323–2343. doi:10.1039/C1CS15188F
55. Paillard A, Passirani C, Saulnier P, et al. Positively-charged, porous, polysaccharide nanoparticles loaded with anionic molecules behave as 'stealth' cationic nanocarriers. *Pharm Res*. 2010;27(1):126–133. doi:10.1007/s11095-009-9986-z
56. Dhandayuthapani B, Yoshida Y, Maekawa T, Kumar DS. Polymeric scaffolds in tissue engineering application: a review. *Int J Polym Sci*. 2011;2011. doi:10.1155/2011/290602
57. Misra S, Hascall VC, Markwald RR, Ghatak S. Interactions between hyaluronan and its receptors (CD44, RHAMM) regulate the activities of inflammation and cancer. *Front Immunol*. 2015;6:201.
58. Ross AE, Tang MY, Gemeinhart RA. Effects of molecular weight and loading on matrix metalloproteinase-2 mediated release from poly (ethylene glycol) diacrylate hydrogels. *AAPS J*. 2012;14(3):482–490. doi:10.1208/s12248-012-9356-3
59. McAvoy K, Jones D, Thakur RRS. Synthesis and characterisation of photocrosslinked poly(ethylene glycol) diacrylate implants for sustained ocular drug delivery. *Pharm Res*. 2018;35(2):36. doi:10.1007/s11095-017-2298-9
60. Caló E, Khutoryanskiy VV. Biomedical applications of hydrogels: a review of patents and commercial products. *Eur Polym J*. 2015;65:252–267. doi:10.1016/j.eurpolymj.2014.11.024
61. Liu HZ, Hao JS, Li KS. Current strategies for drug delivery to the inner ear. *Acta Pharm Sin B*. 2013;3(2):86–96. doi:10.1016/j.apsb.2013.02.003
62. Canalis E, Hott M, Deloffre P, Tsouderos Y, Marie PJ. The divalent strontium salt S12911 enhances bone cell replication and bone formation in vitro. *Bone*. 1996;18(6):517–523. doi:10.1016/8756-3282(96)00080-4
63. Sila-Asna M, Bunyaratvej A, Maeda S, Kitaguchi H, Bunyaratavej N. Osteoblast differentiation and bone formation gene expression in strontium-inducing bone marrow mesenchymal stem cell. *Kobe J Med Sci*. 2007;53(1–2):25–35.
64. Nardone V, Zonefrati R, Mavilia C, et al. In vitro effects of strontium on proliferation and osteoinduction of human preadipocytes. *Stem Cells Int*. 2015;2015:871863. doi:10.1155/2015/871863
65. Orienti I, Zuccari G, Fini A, et al. Modified doxorubicin for improved encapsulation in PVA polymeric micelles. *Drug Deliv*. 2004;12(1):15–20. doi:10.1080/10717540590889574
66. Howell SB. Clinical applications of a novel sustained-release injectable drug delivery system: DepoFoam technology. *Cancer J*. 2001;7(3):219–227.
67. Wei W, Li H, Yin C, Tang F. Research progress in the application of in situ hydrogel system in tumor treatment. *Drug Deliv*. 2020;27(1):460–468. doi:10.1080/10717544.2020.1739171
68. Grumezescu AM. *Multifunctional Systems for Combined Delivery, Biosensing and Diagnostics*. William Andrew; 2017.
69. Andrzejowski P, Giannoudis PV. The 'diamond concept' for long bone non-union management. *J Orthop Traumatol*. 2019;20(1):21. doi:10.1186/s10195-019-0528-0
70. Lee JH, Baek HR, Lee EN, Lee KM, Lee HK. The efficacy of porous hydroxyapatite granule as a carrier of e.coli-derived recombinant human bone morphogenetic protein-2. *Tissue Eng Regen Med*. 2013;10(5):279–285. doi:10.1007/s13770-013-1090-0
71. Wu T, Sun J, Tan L, et al. Enhanced osteogenesis and therapy of osteoporosis using simvastatin loaded hybrid system. *Bioact Mater*. 2020;5(2):348–357. doi:10.1016/j.bioactmat.2020.03.004
72. Rao RD, Bagaria VB, Cooley BC. Posterolateral intertransverse lumbar fusion in a mouse model: surgical anatomy and operative technique. *Spine J*. 2007;7(1):61–67. doi:10.1016/j.spinee.2006.03.004
73. Ferland C, Laverty S, Beaudry F, Vachon P. Gait analysis and pain response of two rodent models of osteoarthritis. *Pharmacol Biochem Behav*. 2011;97(3):603–610. doi:10.1016/j.pbb.2010.11.003
74. Ishikawa G, Nagakura Y, Takeshita N, Shimizu Y. Efficacy of drugs with different mechanisms of action in relieving spontaneous pain at rest and during movement in a rat model of osteoarthritis. *Eur J Pharmacol*. 2014;738:111–117. doi:10.1016/j.ejphar.2014.05.048